# First Principles Calculation of Stress Induced Amorphization in Armor Ceramics

by D. E. Taylor, T. W. Wright, and J. W. McCauley

## NOTICES

### Disclaimers

# Army Research Laboratory
Aberdeen Proving Ground, MD 21005

**ARL-MR-0779**                                      **May 2011**

# First Principles Calculation of Stress Induced Amorphization in Armor Ceramics

**D. E. Taylor and J. W, McCauley**
Weapons and Materials Research Directorate, ARL

**T. W. Wright**
Adjunct Research Professor, Johns Hopkins University

**20110523126**

# REPORT DOCUMENTATION PAGE

**Form Approved**
**OMB No. 0704-0188**

Public reporting burden for this collection of information is estimated to average 1 hour per response, including the time for reviewing instructions, searching existing data sources, gathering and maintaining the data needed, and completing and reviewing the collection information. Send comments regarding this burden estimate or any other aspect of this collection of information, including suggestions for reducing the burden, to Department of Defense, Washington Headquarters Services, Directorate for Information Operations and Reports (0704-0188), 1215 Jefferson Davis Highway, Suite 1204, Arlington, VA 22202-4302. Respondents should be aware that notwithstanding any other provision of law, no person shall be subject to any penalty for failing to comply with a collection of information if it does not display a currently valid OMB control number.
**PLEASE DO NOT RETURN YOUR FORM TO THE ABOVE ADDRESS.**

| 1. REPORT DATE *(DD-MM-YYYY)* | 2. REPORT TYPE | 3. DATES COVERED (From - To) |
|---|---|---|
| May 2011 | DRI | FY10 |

| 4. TITLE AND SUBTITLE | 5a. CONTRACT NUMBER |
|---|---|
| First Principles Calculation of Stress Induced Amorphization in Armor Ceramics | |
| | 5b. GRANT NUMBER |
| | 5c. PROGRAM ELEMENT NUMBER |
| **6. AUTHOR(S)** | 5d. PROJECT NUMBER |
| D. E. Taylor, T. W. Wright, and J. W. McCauley | |
| | 5e. TASK NUMBER |
| | 5f. WORK UNIT NUMBER |

| 7. PERFORMING ORGANIZATION NAME(S) AND ADDRESS(ES) | 8. PERFORMING ORGANIZATION REPORT NUMBER |
|---|---|
| U.S. Army Research Laboratory ATTN: RDRL-WML-B Aberdeen Proving Ground, MD 21005 | ARL-MR-0779 |

| 9. SPONSORING/MONITORING AGENCY NAME(S) AND ADDRESS(ES) | 10. SPONSOR/MONITOR'S ACRONYM(S) |
|---|---|
| | |
| | 11. SPONSOR/MONITOR'S REPORT NUMBER(S) |

**12. DISTRIBUTION/AVAILABILITY STATEMENT**

Approved for public release; distribution unlimited.

**13. SUPPLEMENTARY NOTES**

**14. ABSTRACT**

Recent experimental work within the U.S. Army Research Laboratory has identified the formation of nanoscale-sized intragranular amorphous bands leading to a marked reduction in ballistic performance of boron carbide ($B_4C$). This pressure-induced amorphization has been examined through application of the Born stability criterion that imposes restrictions on the relative magnitudes of the elastic constants of a stable crystal. The analysis has been conducted for $B_4C$ as a function of structural polytype using ab initio solid-state density functional methods and the results of the pressure evolution of the $B_4C$ elastic constants are reported. It is shown that the C-C-C polytype, a minority phase in the $B_4C$ lattice, fails at a pressure of $\approx 20$ gigapascals less than the other polytypes tested in this survey, indicating that it may serve as one of the initial points of failure upon impact.

**15. SUBJECT TERMS**

Boron carbide, amorphization, elastic constant

| 16. SECURITY CLASSIFICATION OF: | | | 17. LIMITATION OF ABSTRACT | 18. NUMBER OF PAGES | 19a. NAME OF RESPONSIBLE PERSON D. E. Taylor |
|---|---|---|---|---|---|
| a. REPORT | b. ABSTRACT | c. THIS PAGE | UU | 24 | 19b. TELEPHONE NUMBER *(Include area code)* |
| Unclassified | Unclassified | Unclassified | | | (410) 306-0853 |

Standard Form 298 (Rev. 8/98)
Prescribed by ANSI Std. Z39.18

ii

# Contents

# List of Figures

# List of Tables

# Acknowledgments

INTENTIONALLY LEFT BLANK.

# 1. Objective

Boron carbide (BC), due to its extreme hardness and low density, has been used as an armor ceramic for many years. Its elastic properties, which surpass more dense compounds such as silicon carbide by a factor of 2, suggest that BC should sustain high impact pressures without failure; however, there is an anomalous loss of impact resistance within the material, apparently due to increased fragmentation by a factor of 2 to 3. Recent experimental work within the U.S. Army Research Laboratory has identified the formation of nanoscale-sized intragranular amorphous bands as the primary damage mechanism leading to the marked reduction in ballistic performance of BC (1, 2). The Army has a need to understand the mechanism for the formation of these amorphous bands, *at the atomic level*, which will allow for the design of chemically modified BC materials that will show improved impact resistance and, hence, improved armor ceramic performance. Using first principles quantum mechanics, we provide much needed insight into the formation mechanism of the experimentally observed amorphous bands that are known to weaken BC ceramics. In particular, the stress-induced amorphization of BC is explored via application of the "Born instability" criterion, which requires that the matrix of second derivatives of the energy per unit cell be positive definite, where the six independent variables are strain measures in the current configuration. A material that exhibits a Born instability loses its ability (at some stress and temperature) to convert certain incremental strain patterns into stress increments. These strain patterns are known as "soft" modes of deformation, which must be related to movements within the atomic structure. Identification of the onset and nature of the Born instability will give further insight into the formation mechanism of the amorphous regions that weaken the BC material. In this research, we examine the influence of both pressure and shear stress on the Born instability.

# 2. Approach

BC, with nominal stoichiometry $B_4C$, consists of 12-atom icosahedra crosslinked by 3-atom chains (figure 1) and belongs to the crystallographic space group R-3m (3). The exact nature of the 3-atom chain is unknown experimentally due to the close spectroscopic signatures of boron and carbon. The crystal structure consists of a mixture of $B_{12}$ icosahedra linked by C-C-C chains and $B_{11}C$ icosahedra linked with C-B-C chains (among others). For the C-B-C "polytype," there is an additional complication; the location of the carbon atom in the $B_{11}C$ cage is not known. This, again, is due to the difficulty in definitively resolving boron and carbon; therefore, the carbon atom inserted into the cage could reside in one of two symmetry unique centers, the so-called *polar* and *equatorial* sites within the icosahedron, as shown in figure 1. It should be noted that although BC is generally regarded to have R-3m symmetry, this is only true for the C-C-C

polytype and placement of a carbon atom within the icosahedra causes a distortion of the rhombohedral lattice and the actual structure is dictated by an averaging of all the different polytypes.
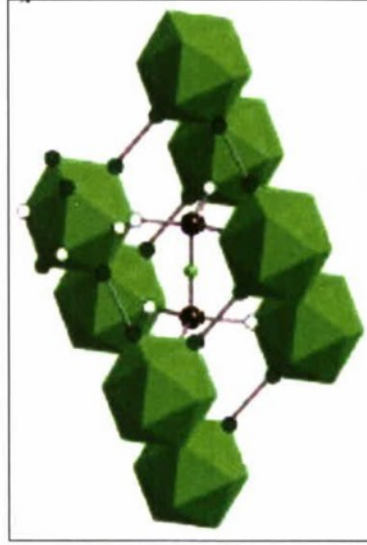


Figure 1. Icosahedral structure of BC. Polar and
equatorial sites in the icosahedra are indicated
by dark green and white spheres, respectively.

As a route to the elucidation of the mechanism by which pressure and shear induce an amorphous transition in BC, we have applied the Born-stability criterion to each of the three polytypes discussed earlier. Born showed that an expansion of the internal energy of a crystal in a power series in the strain, along with the imposition of positivity of the energy, leads to restrictions on the relative magnitudes of the elastic constants of a stable crystal (4). The existence of such a Born instability can be determined quantum mechanically.

BC is highly anisotropic elastically and for crystals with R-3m symmetry, there are only six non-zero independent elastic constants $\{C_{ij}\}$ for the unloaded material (5). These constants have been determined experimentally for BC, except for the modulus $c_{14}$ (6). Each of the elastic moduli varies independently with pressure, and at some point, the system may reach a structural instability. Imposition of the Born stability conditions leads to the following restrictions on the elastic constants for a stable crystal with R-3m symmetry:

$$C_{11} - |C_{12}| > 0 \tag{1}$$

$$(C_{11} + C_{12})C_{33} - 2C_{13}*C_{13} > 0 \tag{2}$$

$$(C_{11} - C_{12})C_{44} - 2C_{14}*C_{14} > 0 \tag{3}$$

The procedure previously adopted by others is to compute the six elastic constants above as a function of pressure and evaluate equations 1 through 3 to determine the onset of the instability, i.e., the pressure at which one or more of the equations above are no longer valid (7, 8). Once

2

the initial instability has been located, evaluation of the "soft modes" of deformation (atomic displacements corresponding to the instability) can be determined.

Equations 1–3 are generally not applicable to the incremental moduli of crystals under finite loading; however, a general indicator of an elastic instability for all materials under any state of loading is

$$\det | \mathbf{C} | = 0, \tag{4}$$

where $\mathbf{C}$ is the full 6x6 tensor of incremental elastic moduli (9, 10). Further, since the determinant of a matrix is equal to the product of its eigenvalues, an equivalent statement of equation 4 is that all the eigenvalues of $\mathbf{C}$ must be positive and the first stress state at which an eigenvalue equals zero corresponds to an instability. It should be noted that for a crystal under load, the elastic constant tensor $\mathbf{C}$ should be replaced by the "effective" elastic constant tensor $\mathbf{B}$ given by

$$B_{ijkl} = C_{ijkl} + (1/2)(\delta_{ik}\tau_{jl} + \delta_{jk}\tau_{il} + \delta_{il}\tau_{jk} + \delta_{jl}\tau_{ik} - 2\delta_{kl}\tau_{ij}) \tag{5}$$

with $\tau_{ij}$ being an element of the stress tensor (10).

The elastic constants were computed using the CP2K software package (11). Density functional theory using the Perdew-Burke-Ernzerhof (PBE) functional (12) in a double zeta valence plus polarization basis set was used for all calculations with a planewave cutoff of 800 Rydberg. Elastic constants are related to the second derivative of the total energy with respect to strain, $\varepsilon_i$, via

$$C_{ij} = \frac{1}{V}\frac{\partial^2 E}{\partial\varepsilon_i\partial\varepsilon_j}\bigg|_0 , \tag{6}$$

where V is the unit cell volume and i,j=1…6 in the Voigt notation (13). The CP2K software does not evaluate elastic constants analytically; therefore, a Fortran program was written for this work that evaluates the second derivative of the energy with respect to strain (equation 6) via a finite difference of analytic first derivatives provided by the CP2K code. This new program includes the required stress corrections from equation 5 in the computation of the elastic constants, computes the bulk modulus using the Voigt-Reuss-Hill approximation (14), and finally determines the eigenspectrum of the elastic tensor. Since we have used the finite difference approach, the *full* 6x6 elastic constant tensor can be evaluated with only 6 quantum mechanical (QM) calculations (12 if double-sided differences are taken, as is done in this work). This is much less than the *minimum* 43 calculations required using a strain energy approach advocated by some authors.

3

# 3. Results

The optimized lattice parameters for each polytype are presented in table 1. The theoretical structures computed using PBE are in excellent agreement with experiment (*3*) and the distortion of the lattice from purely rhombohedral symmetry is clearly evident in the polar and equatorial polytypes. Lazzari et al. conducted a computational study and concluded that the polar polytype is the most stable configuration energetically (*15*). This is also supported by our results where it is found that the C-C-C and equatorial polytypes lie 71 and 35 meV/atom higher in energy than the polar configuration, respectively.

Table 1. Unit cell parameters of BC polytypes (lengths in angstrom, angles in degrees volume in cubic angstroms).

| Polytype | a | b | c | alpha | beta | gamma | Volume |
|----------|------|------|------|-------|-------|-------|--------|
| CCC | 5.196 | 5.196 | 5.196 | 66.00 | 66.00 | 66.00 | 112.12 |
| Polar | 5.070 | 5.215 | 5.215 | 65.24 | 66.07 | 66.07 | 109.75 |
| Equatorial | 5.176 | 5.213 | 5.213 | 64.87 | 64.96 | 64.96 | 110.17 |
| Experiment | 5.19 | 5.19 | 5.19 | 65.18 | 65.18 | 65.18 | 110.02 |

Each polytype was subjected to hydrostatic compression and the resulting pressure-volume data was fitted to the third order Birch-Murnaghan equation of state (*16*). As shown in figure 2, the pressure response of each polytype is very similar. The computed bulk moduli for each polytype (and its associated pressure derivative resulting from the Birch-Murnaghan fit) are presented in table 2 and compare exceptionally well with the experimental value. The polar and equatorial polytypes, both with C-B-C chains, have bulk moduli that are marginally different; however, the C-C-C polytype has a reduction of ≈12 GPa, indicating that it is softer than the other polytypes. It has been suggested that the C-C-C polytype, a minority phase in the BC crystal, is the "weakest link" in the structure and may be the polytype that fails first when impacted. The lower bulk modulus is in support of that hypothesis however more rigorous evidence will be provided in the following.
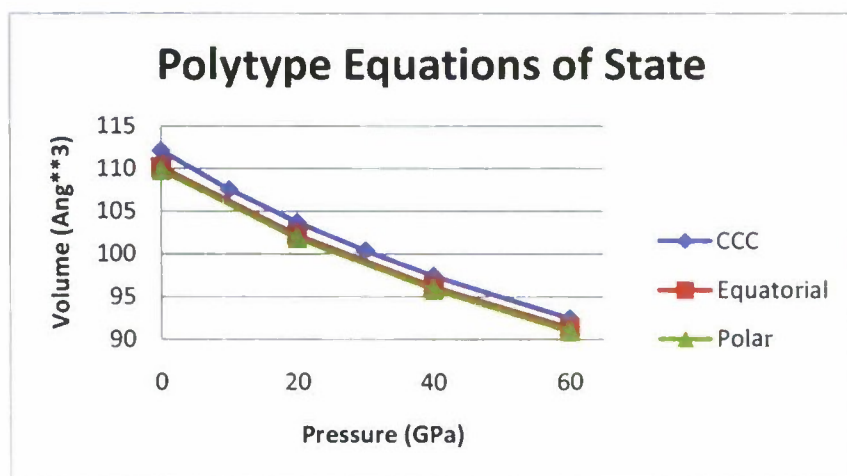
Figure 2. Equations of state for each polytype.

Table 2. Bulk modulus and pressure derivative resulting from Birch-Murnaghan equation of state fit to DFT data.

| Polytype | Bulk Modulus (GPa) | Pressure Derivative |
|---|---|---|
| CCC | 222 | 3.5 |
| Polar | 234 | 3.3 |
| Equatorial | 233 | 3.4 |
| Experiment | 236 | |

The elastic moduli of BC have been evaluated experimentally by McClellan et al. (6); however, in their analysis, they assumed a hexagonal symmetry (due to limitations in their fitting software), which leaves the value of the $C_{14}$ elastic constant indeterminate (5). Since elastic constants are tensor quantities that depend on orientation, *in order to have a direct comparison with experiment,* we have used a hexagonal setting of the rhombohedral BC unit cell in the initial QM calculations. This does not change any of the conclusions resulting from the stability analysis since the eigenvalues are invariant to any orthogonal transformation of the coordinate axes; it simply allows us to use the experimental values as a metric by which the accuracy of our computed elastic constants can be measured. (We have computed values for $C_{14}$ using the proper rhombohedral setting, however.) The theoretical and experimental elastic constants are presented in table 3. The agreement with experimental values is excellent; however, it should be noted that our theoretical values are for idealized structures with perfect $B_4C$ stoichiometry, whereas the experimental values were obtained from single crystalline measurements of a sample with stoichiometry $B_{5.6}C$ (6). This will invariably affect the experimental results as compared to a perfect $B_4C$ stoichiometry, though it is not clear to what extent.

The pressure evolution of the elastic constants over the 0–80 GPa range for each polytype is shown in figure 3. There we show, for the first time, that for the BC ceramic each $C_{ij}$ increases with pressure however the $C_{44}$ and $C_{66}$ moduli show a marked decrease. This pressure softening of elastic moduli ($C_{44}$ in particular) has been observed experimentally (as well as theoretically) in alpha quartz which is known to undergo pressure induced amorphization similar to the phenomenon observed in BC.

Table 3. Theoretical and experimental elastic constants (GPa).
(The non-zero $C_{14}$ modulus is indeterminate in this orientation.)

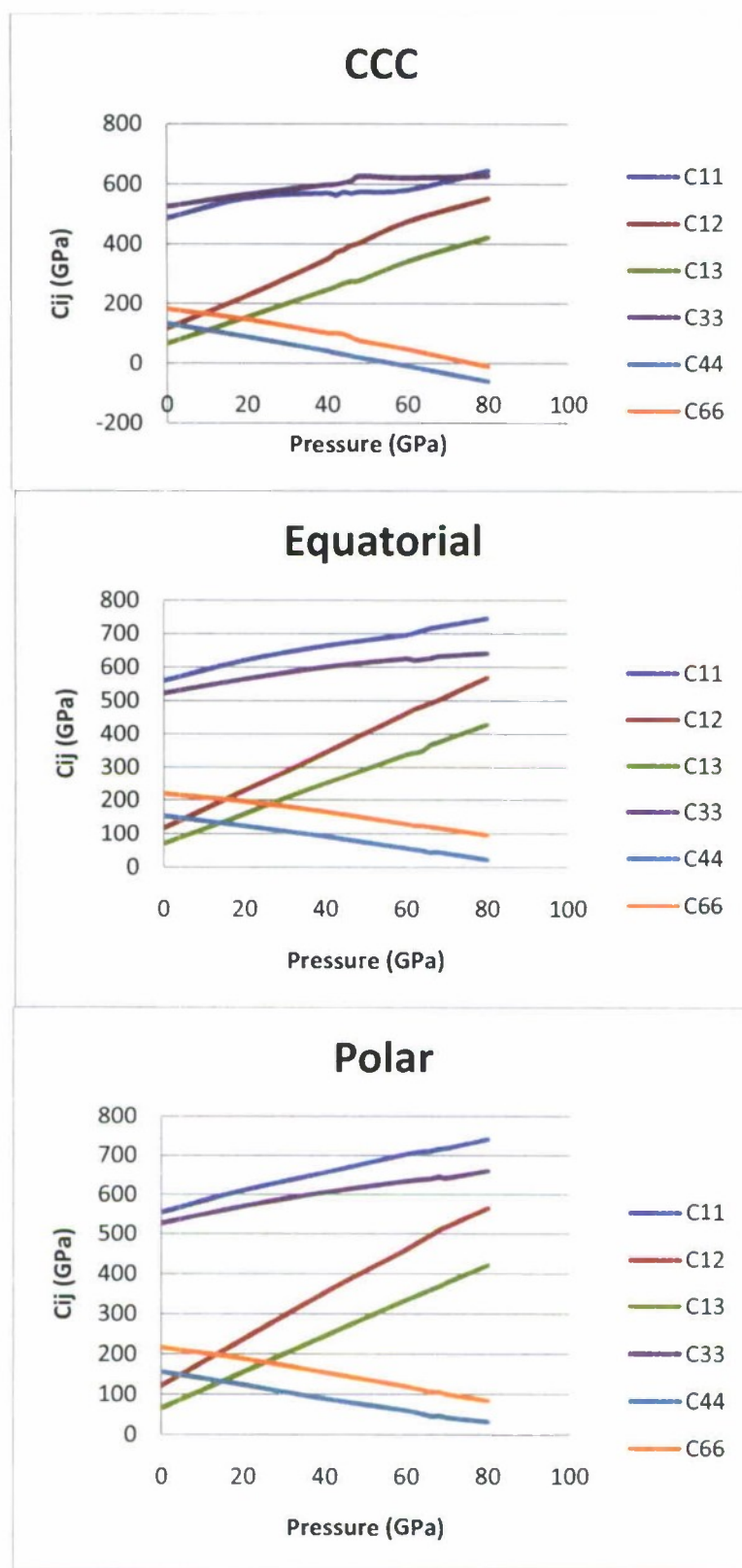| Cij | CCC | Polar | Equatorial | Exp. |
|-----|-----|-------|------------|------|
| C11 | 487 | 554 | 559 | 543 |
| C12 | 117 | 121 | 117 | 131 |
| C13 | 66 | 65 | 70 | 64 |
| C33 | 525 | 526 | 521 | 535 |
| C44 | 133 | 155 | 153 | 165 |
| C66 | 183 | 216 | 218 | 206 |

Figure 3. Pressure evolution of the elastic moduli for each polytype.

The lowest eigenvalue of the elastic constant tensor for each polytype is plotted as a function of pressure in figure 4. For each polytype the eigenvalue decreases monotonically towards zero and reaches zero between 44–46 GPa for the C-C-C polytype and between 66–68 and 68–70 GPa for the equatorial and polar polytypes, respectively, indicating that the C-C-C polytype reaches an elastic instability at much lower pressures than the other polytypes and is the initial point of failure in the BC ceramic under hydrostatic loading. This is in support of the work of Fanchini et al., who studied the stability of BC polytypes relative to the segregated boron and carbon phases (17). In their work they demonstrated that the C-C-C polytype is relatively unstable energetically as compared to the polar and equatorial configurations as a function of hydrostatic load.
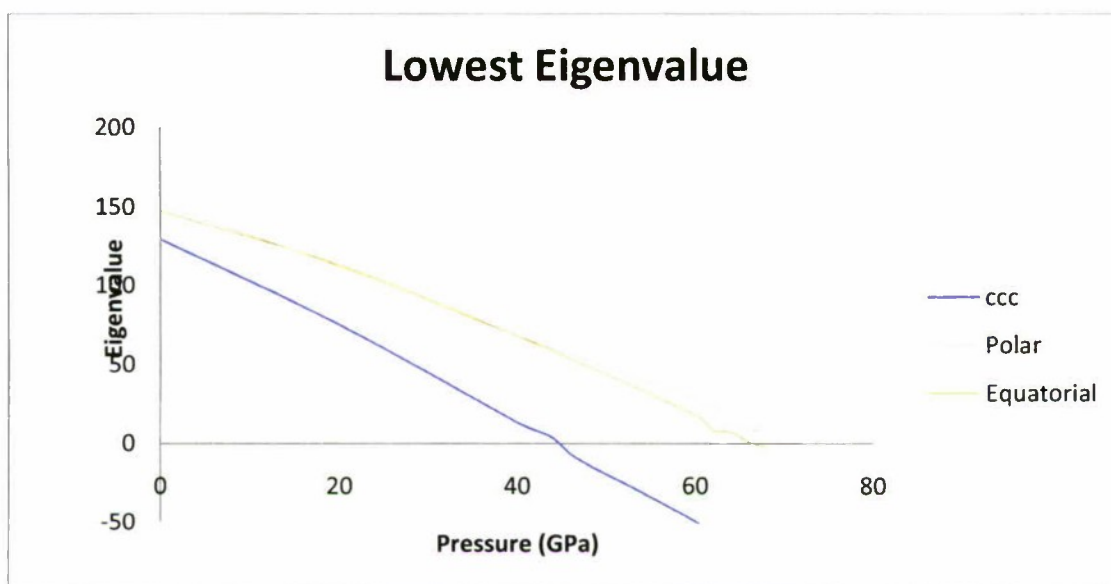


Figure 4. Lowest eigenvalue of elastic constant tensor for each polytype.

## 4. Conclusions

Our calculations thus far have outlined the mechanical response of BC under hydrostatic compression as a function of polytype; however, it has been suggested that shear plays a critical role in weakening the BC ceramic. Our preliminary results lend support to this hypothesis. Specifically, examination of the eigenvectors associated with the soft mode eigenvalues plotted in figure 4 show a significant contribution from shear and indicates that loading along these shearing modes may hasten amorphization. Future work will attempt to construct an amorphization contour in a selected two-dimensional (2-D) pressure—shear space. It now appears feasible to use theoretical constitutive representations from nonlinear elasticity to minimize the QM calculations so that full exploration of the six-dimensional (6-D) stress space is unnecessary.

8

The stability analysis conducted herein allows for identification of the stress at which amorphization may initiate; however, one of our ultimate goals is to relate changes in the local atomic structure to the root cause of the instability. For example, Binggeli et al. (7) studied the pressure-induced amorphization phenomenon in α-quartz and presented evidence that a shear instability was the driving force toward collapse of the material. Specifically, when subjected to shear, silicon atoms were displaced towards oxygen atoms, leading to a change in silicon coordination. Previous theoretical work on BC showed that under uniaxial loading the icosahedra remain relatively unaltered; however, there *was* a bending of the 3-atom chain that eventually led to the formation of new covalent bonds between the chain atoms and boron atoms in the icosahedra (18). This type of structural rearrangement can lead to an irreversible alteration of the lattice, which may trigger the collapse of BC leading to amorphization. This rearrangement mechanism needs further study and molecular dynamics simulation, where the change in structural morphology can be studied in real time, is an ideal method for this analysis. However, this is entirely contingent upon the availability of an accurate interatomic potential applicable to BC.

This work has shown that the C-C-C polytype is in fact the weakest polytype within the BC structure; however, these results are based on idealized structures with perfect $B_4C$ stoichiometry. In the actual material, there is a high degree of substitutional disorder as well as defect sites consisting of vacancies in the atomic chain linking the icosahedra. A computational survey of the possible defect polytypes within BC has been conducted by Saal et al. (19); however, their worked focused on structure, enthalpy of formation, and phonon spectra. Therefore, calculations of the mechanical properties of these additional structures are required for a complete stability analysis of the BC ceramic.

# 5. References

1. Moynihan, T. J.; LaSalvia, J. C.; Burkins, M. S. Analysis of Shatter Gap Phenomenon in a $B_4C$/Composite Laminate Armor System. *20th ISB*, Orlando, FL. 23–27 Sept. 2002.

2. Chen, M.; McCauley, J. W.; Hemker, K. J. Shock-induced Localized Amorphization in Boron Carbide. *Science* **2003**, *299*, 1563.

3. Clark, H. K.; Hoard, J. L. The Crystal Structure of Boron Carbide. *J. Am. Cer. Soc* **1943**, *65*, 2115.

4. Born, M.; Huang, K. *Dynamical Theory of Crystal Lattices*; Oxford University Press: London, 1954.

5. Nye, J. F. *Physical Properties of Crystals*; Oxford at the Clarendon Press, (1957).

6. McClellan, K. J.; Chu, F.; Roper, J. M.; Shindo l. Room Temperature Single Crystal Elastic Constants of Boron Carbide. *J. Mat. Sci.* **2001**, *36*, 3403.

7. Binggeli, N.; Chelikowsky, J. R. Elastic Instability in α-Quartz Under Pressure. *Phys. Rev. Lett.* **1992**, *69*, 2220.

8. Tse, J. S.; Klug, D. D. Mechanical Instability of α-Quartz: A Molecular Dynamics Study. *ibid* **1991**, *67*, 3559.

9. Wang, J.; Li, J.; Yip, S. Mechanical Instabilities of Homogenous Crystals. *Phys. Rev. B* **1995**, *52*, 12627.

10. Wang, J.; Yip, S.; Phillpot, S. R.; Wolf, D. Crystal Instabilities at Finite Strain. *Phys. Rev. Lett.* **1993**, *71*, 4182.

11. CP2K is freely available from http://cp2k.berlios.de/ (accessed January, 2010).

12. Perdew, J. P.; Burke, K.; Ernzerhof, M. Generalized Gradient Approximation Made Simple. *Phys. Rev. Lett.* **1996**, *77*, 3865.

13. Perger, W. F.; Criswell, J.; Civalleri, B.; Dovesi, R. Ab Initio Calculation of Elastic Constants of Crystalline Systems with the CRYSTAL Code. *Comp. Phys. Comm.* **2009**, *180*, 1753.

14. Hill, R. The Elastic Behaviour of a Crystalline Aggregate. *Proc. of the Phys. Soc. A* **1952**, *65*, 349.

15. Lazzari, R.; Vast, N.; Besson, J. M.; Baroni, S.; Dal Carso, A. Atomic Structure and Vibrational Properties of Icosahedral $B_4C$ Boron Carbide. *Phys. Rev. Lett.* **1999**, *83*, 3230.

16. Birch, F.  Finite Elastic Strain of Cubic Crystals.  *Phys. Rev.* **1947**, *71*, 809.

17. Fanchini, G.; McCauley, J. W.; Chhowalla, M.  Behavior of Disordered Boron Carbide Under Stress.  *Phys. Rev. Lett.* **2006**, *97*, 035502.

18. Yan, X. Q.; Tang, Z.; Zhang, L.; Guo, J. J.; Jin, C. Q.; Zhang, Y.; Goto, T.; McCauley, J. W.; Chen, M. W.  Depressurization Amorphization of Single-Crystal Boron Carbide. *ibid* **2009**, *102*, 075505.

19. Saal, J. E.; Shang, S.; Liu, Z.  The Structural Evolution of Boron Carbide Via Ab Initio Calculations.  *App. Phys. Lett.* **2007**, *91*, 231915.

## 6. Transitions

Results of this work will be presented at the 35th International Conference and Exposition on Advanced Ceramics and Composites (Taylor, 2011) and at the American Society of Mechanical Engineers (ASME) Applied Mechanics and Materials Conference (Wright, 2011).

2       CALTECH
        G RAVICHANDRAN
        T AHRENS MS 252 21
        1201 E CALIFORNIA BLVD
        PASADENA CA 91125

5       SOUTHWEST RSRCH INST
        C ANDERSON
        K DANNEMANN
        T HOLMQUIST
        G JOHNSON
        J WALKER
        PO DRAWER 28510
        SAN ANTONIO TX 78284

3       SRI INTERNATIONAL
        D CURRAN
        D SHOCKEY
        R KLOOP
        333 RAVENSWOOD AVE
        MENLO PARK CA 94025

1       APPLIED RSRCH ASSOCIATES
        D GRADY
        4300 SAN MATEO BLVD NE
        STE A220
        ALBUQUERQUE NM 87110

1       INTERNATIONAL RSRCH
        ASSOCIATES INC
        D ORPHAL
        4450 BLACK AVE
        PLEASANTON CA 94566

1       BOB SKAGGS CONSULTANT
        S R SKAGGS
        7 CAMINO DE LOS GARDUNOS
        SANTA FE NM 87501

2       WASHINGTON ST UNIV
        INST OF SHOCK PHYSICS
        Y GUPTA
        J ASAY
        PULLMAN WA 99164-2814

1       COORS CERAMIC CO
        T RILEY
        600 NINTH ST
        GOLDEN CO 80401

1       UNIV OF DAYTON
        RSRCH INST
        N BRAR
        300 COLLEGE PARK
        MS SPC 1911
        DAYTON OH 45469-0168

2       COMMANDER
        US ARMY TACOM
        AMSTA TR S
        T FURMANIAK
        L PROKURAT FRANKS
        WARREN MI 48397-5000

1       PROJECT MANAGER
        ABRAMS TANK SYSTEM
        J ROWE
        WARREN MI 48397-5000

3       COMMANDER
        US ARMY RSRCH OFC
        B LAMATINA
        D STEPP
        W MULLINS
        PO BOX 12211
        RSRCH TRIANGLE PARK NC
        27709-2211

1       NAVAL SURFACE WARFARE CTR
        CARDEROCK DIVISION
        R PETERSON
        CODE 28
        9500 MACARTHUR BLVD
        WEST BETHESDA MD 20817-5700

4       LAWRENCE LIVERMORE NATL LAB
        R GOGOLEWSKI L290
        R LANDINGHAM L369
        J E REAUGH L282
        S DETERESA
        PO BOX 808
        LIVERMORE CA 94550

4       SANDIA NATL LAB
        J ASAY MS 0548
        L CHHABILDAS MS 0821
        D CRAWFORD ORG 0821
        M KIPP MS 0820
        PO BOX 5800
        ALBUQUERQUE NM 87185-0820

| | | | |
|---|---|---|---|
| 3 | RUTGERS<br>THE STATE UNIV OF NEW JERSEY<br>DEPT OF CRMCS & MATLS ENGRNG<br>R HABER<br>607 TAYLOR RD<br>PISCATAWAY NJ 08854 | 2 | CERADYNE INC<br>M NORMANDIA<br>3169 REDHILL AVE<br>COSTA MESA CA 96626 |
| 2 | THE UNIVERSITY OF TEXAS<br>AT AUSTIN<br>S BLESS<br>IAT<br>3925 W BRAKER LN STE 400<br>AUSTIN TX 78759-5316 | 3 | JOHNS HOPKINS UNIV<br>DEPT OF MECH ENGRNG<br>K T RAMESH<br>T W Wright<br>3400 CHARLES ST<br>BALTIMORE MD 21218 |
| 3 | SOUTHWEST RSRCH INST<br>C ANDERSON<br>J RIEGEL<br>J WALKER<br>6220 CULEBRA RD<br>SAN ANTONIO TX 78238 | 2 | SIMULA INC<br>V HORVATICH<br>V KELSEY<br>10016 51ST ST<br>PHOENIX AZ 85044 |
| 1 | CERCOM<br>R PALICKA<br>991 PARK CENTER DR<br>VISTA CA 92083 | 3 | UNITED DEFENSE LP<br>E BRADY<br>R JENKINS<br>K STRITTMATTER<br>PO BOX 15512<br>YORK PA 17405-1512 |
| 6 | GDLS<br>W BURKE MZ436 21 24<br>G CAMPBELL MZ436 30 44<br>D DEBUSSCHER MZ436 20 29<br>J ERIDON MZ436 21 24<br>W HERMAN MZ435 01 24<br>S PENTESCU MZ436 21 24<br>38500 MOUND RD<br>STERLING HTS MI 48310-3200 | 10 | NATL INST OF STANDARDS & TECH<br>CRMCS DIV<br>G QUINN<br>STOP 852<br>GAITHERSBURG MD 20899 |
| 1 | INTERNATL RSRCH ASSN<br>D ORPHAL<br>4450 BLACK AVE<br>PLEASANTON CA 94566 | 2 | DIR USARL<br>AMSRD ARL D<br>C CHABALOWSKI<br>V WEISS<br>2800 POWDER MILL RD<br>ADELPHI MD 20783-1197 |
| 1 | JET PROPULSION LAB<br>IMPACT PHYSICS GROUP<br>M ADAMS<br>4800 OAK GROVE DR<br>PASADENA CA 91109-8099 | | |
| 3 | OGARA HESS & EISENHARDT<br>G ALLEN<br>D MALONE<br>T RUSSELL<br>9113 LE SAINT DR<br>FAIRFIELD OH 45014 | | |

NO. OF
COPIES   ORGANIZATION

ABERDEEN PROVING GROUND

65      DIR USARL
        RDRL WM
          S KARNA
          J MCCAULEY (10 CPS)
          J SMITH
        RDRL WMB
          J NEWILL
          M ZOLTOSKI
          D TAYLOR (10 CPS)
        RDRL WMM
          S MCKNIGHT
          R DOWDING
        RDRL WMM C
          R SQUILLACIOTI
        RDRL WMM D
          E CHIN
          K CHO
          G GAZONAS
          J LASALVIA
          P PATEL
          J MONTGOMERY
          J SANDS
        RDRL WMS
          T JONES
        RDRL WMT
          P BAKER
          B BURNS
        RDRL WMT A
          P BARTKOWSKI
          M BURKINS
          W GOOCH
          D HACKBARTH
          T HAVEL
          C HOPPEL
          E HORWATH
          M KEELE
          D KLEPONIS
          H MEYER
          J RUNYEON
          S SCHOENFELD
        RDRL WMT C
          T BJERKE
          T FARRAND
          K KIMSEY
          L MAGNESS
          S SEGLETES
          D SCHEFFLER
          R SUMMERS
          W WALTERS

        RDRL WMT D
          J CLAYTON
          D DANDEKAR
          M GREENFIELD
          E RAPACKI
          M SCHEIDLER
          T WEERASOORIYA
        RDRL SL
          R COATES